

A New Measure of Circularity Based on Distribution of the Radius

Ana M. Herrera-Navarro¹, Hugo Jiménez Hernández², Hayde Peregrina-Barreto¹,
Federico Manríquez- Guerrero³, and Iván R. Terol-Villalobos³

¹ Facultad de Ingeniería, Universidad Autónoma de Querétaro, Querétaro,
Mexico

² Centro de Ingeniería y Desarrollo Industrial, Querétaro,
Mexico

³ Centro de Investigación y Desarrollo Tecnológico en Electroquímica, Querétaro,
Mexico

anaherreranavarro@gmail.com, hugo.jimenez@cidesi.mx, hperegrina@ieee.org,
fmanriquez@cideteq.mx, famter@ciateq.mx

Abstract. The measures most commonly used in current literature to compute the roundness of digital objects are derivations of the form factor based on area and perimeter computations. However, these measures are highly dependent on image resolution and sensitive to shape variations. In this article, a new measure is proposed. This measure takes into consideration the dominant geometry of objects, avoiding the use of such parameters as area, perimeter and Ferret's diameter. The proposed measure is easy to compute, and since it is a distribution of probability based on the radius, it is invariant to abrupt changes in contours or to shape resolution. In order to show the performance of this measure, it is compared with three other recently proposed measures: factor shape, which is recommended by the American Standard Test Measurement, mean roundness and radius ratio.

Keywords. Measure, shape, circularity, probability density function, center, radius, medium, mode.

Una nueva medida de circularidad basada en la distribución de radios

Resumen. Las medidas de circularidad más utilizadas en la literatura actual para calcular la redondez de objetos digitales son derivaciones del factor de forma, que se basa en el área y perímetro. Sin embargo, estas medidas son altamente dependientes de la resolución de la imagen y sensibles a variaciones de forma. En este artículo se propone una nueva medida de circularidad que considera la geometría dominante de los objetos, evitando el uso de parámetros como área, perímetro y diámetro de Ferret. La medida propuesta tiene una complejidad computacional baja, y debido a

que es basada en la distribución de probabilidad de los radios, no es afectada por cambios bruscos en los contornos o forma de resolución. Para mostrar el comportamiento de la medida, esta es comparada con otras tres medidas recientemente propuestas: factor de forma, la cual es recomendada por la medición de estándar americano de pruebas y materiales, redondez media y la relación de radio.

Palabras clave. Medida, forma, circularidad, función de densidad de probabilidad, centro, radio, media, moda.

1 Introduction

Shape characterization is an ongoing research topic, especially in digital image processing and discrete geometry [5, 22, 32, 33]. For instance, the measurement of circularity is a subject of interest in many fields of applications such as medicine and industrial processes [12, 15, 8, 11, 2, 10, 25]. In particular, circularity plays an important role in materials science as a way to understand the mechanical properties of ductile cast iron [23, 13, 27]. The most widely used measure of circularity in current literature is the so-called shape factor (SF) given by $SF = 4\pi Area/P^2$ [34], where P is the perimeter. The main problem associated with this measure consists in its dependence on image resolution and perimeter inaccuracy. In addition, it is theoretically unsatisfactory because digital circles may have different values which are less than 1

[30]. These drawbacks have motivated the design of other circularity measures. In summary, the approaches found in the literature to compute the circularity can be classified in four main groups as follows.

(i) Approaches based on the circular Hough Transformation (HT) [35, 24, 36]: these are robust to noise, as well as to shape distortions and to occlusions/missing parts of an object. Their main disadvantages are computational complexity and storage requirements of the algorithms, which increase exponentially to the dimensionality of the curve. This means that for straight lines the computational complexity and storage requirements are close to $O(n^2)$ and for circles, to $O(n^3)$.

(ii) Approaches based on the separation of the circle problem into discrete and computational geometry [37, 26]: these approaches allow the recognition of digital arcs. These algorithms need to be extended to measure the extent of the deviation with a digital arc.

(iii) Approaches based on the shape templates [28, 6, 26, 38]: these methods compare parameters of an object with a circle in the Euclidean plane. These approximations have a number of drawbacks. First, the generation of a digitized disk adds more complexity. Second, it is necessary to know the real object to generate a digitized disk according to the shape resolution.

(iv) Approaches based on circle fitting [1, 16, 9]: a circle is fitted to a set of pixels with the least square norm. In some cases these methods offer solution with a minimum error, but they do not necessarily provide the best solution to the data, because they do not consider data aberrations.

The aforementioned approaches represent different attempts to characterize circularity. However, these measures are affected when the resolution of a digital region is changed. Furthermore, they are affected by noise (unsharpened borders). Recently, Ritter and Cooper [30] reviewed and compared seven measures of circularity in terms of resolution dependence, demonstrating that most of them are derivations of SF. In their work, the authors proposed two new measures of roundness: the mean roundness (MR) and the radius ratio (RR). These measures can be useful to assess the circularity of regular objects in a two-dimensional

space; however, when the information of an object is given partially or there are abrupt changes in the contours, they become inefficient. On the other hand, several properties can be found in the literature that maybe useful for constructing a good measure of circularity for digital figures. One of the most representative measures was proposed by Haralick [34]. In his work, the author discovered four properties:

- (i) the more circular a figure becomes, the more the measure of its circularity increases;
- (ii) the values for digital figures follow the values for the corresponding continuous figures;
- (iii) the circularity measure is independent of orientation; and
- (iv) the circularity measure is area independent.

In this paper, we present a new measure of circularity which, having the four properties mentioned above, satisfy the following desirable conditions:

1. It is independent of different resolutions.
2. It is tolerant to shape variations (including deformations).
3. It is robust against noise.
4. It ranges within $[0,1]$, where 1 is scored only by a perfect circle.
5. It can be easily compared to human perception.
6. It is intuitive, i.e., it is expected to increase as the number of sides of a regular polygon increases.

The rest of the paper is organized as follows. In Section 2, a brief description of three measures is provided: radius ratio (RR), mean roundness (MR) and roundness factor (RF), together with their performance and limitations. In Section 3, a new discrete measure based on the distribution of the radius is proposed. Some illustrative examples, demonstrating the fact that the distribution of the distances from the border points to the center of nodules can be modeled as a multimodal probabilistic distribution function (pdf), are also featured in Section 4. In Section 5, an experimental study is carried out to compare the proposed measure with the measures that were previously described. Finally, comments and conclusions are given.

2 Review of Roundness Measures

A measure recommended by the American Society for Testing and Materials (ASTM) to compute circularity is ASTM circularity [3, 20]. Although this measure has been applied using different names, in this work it will be called roundness factor. This measure is based on the area of a circumscribed circle with the same maximum diameter of an object and is defined as

$$RF = \frac{4Area}{\pi F_{max}^2}, \quad (1)$$

where F_{max} is the maximum of Ferret's diameter (the longest distance between two points along the boundary of an object). The main disadvantage in using this parameter consists in small variations in shape, sometimes seen as fine peaks, which strongly affect the results of roundness, even when the object being evaluated has a well-defined circular shape. In such cases, the maximum Ferret's diameter is larger than the diameter of the inscribed circle. It was demonstrated in [20] that parameters such as Ferret's diameter differ up to 30 percent within image analysis tests of various image processing systems.

On the other hand, recently, Ritter and Cooper

[30] reviewed and compared several measures of circularity in terms of resolution, order of complexity, ease of calculation, and how well they match human observations. This article shows that most circularity measures are derivations of the form factor. The main problem associated with this measure is its dependence on resolution and perimeter inaccuracy. Besides, it requires the identification of both the border and the interior points of the object. To overcome this problem, the authors propose two measures of roundness: the mean roundness and the radius ratio, which are described in the following paragraphs.

The radius ratio measure is based on the definition of a circle. It computes the proportion of the minimum and the maximum radii of the object, as follows:

$$RR = \frac{rb_{min}}{rb_{max}}, \quad (2)$$

where rb_{min} is the minimum radius from a border point to the center of the border, and rb_{max} is the maximum radius. The main disadvantage of this measure is that the proportions of the shortest and longest radii do not provide sufficient information to characterize the roundness, and it can be affected by pixel aberrations as well.

The mean roundness measure is based on the theory of mean deviation [4]; it calculates the sum of the absolute differences between the radius of

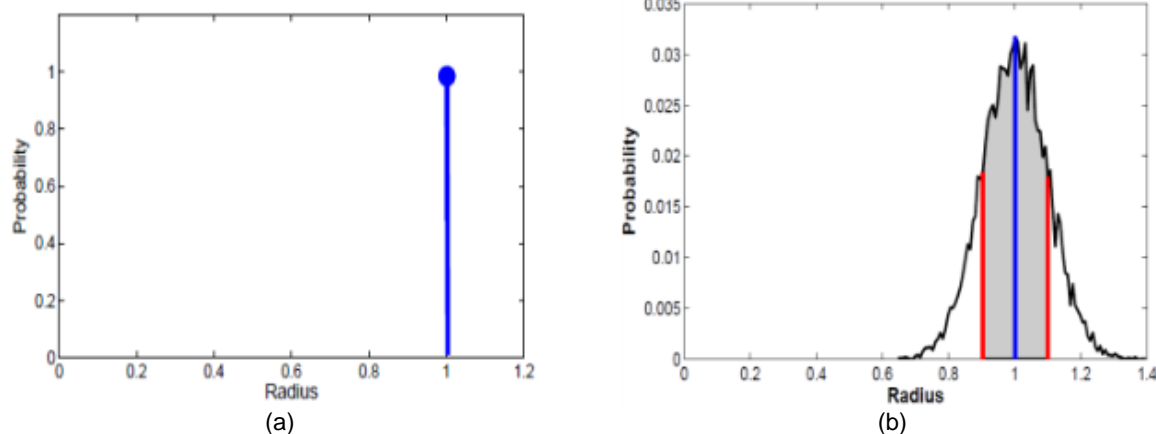


Fig. 1. Probability distribution function of the radius corresponding to (a) an ideal circumference, where pdf becomes only a peak located at the radius; and (b) a deformed circumference, the majority of the area is clustered around the maximum which represents the radius

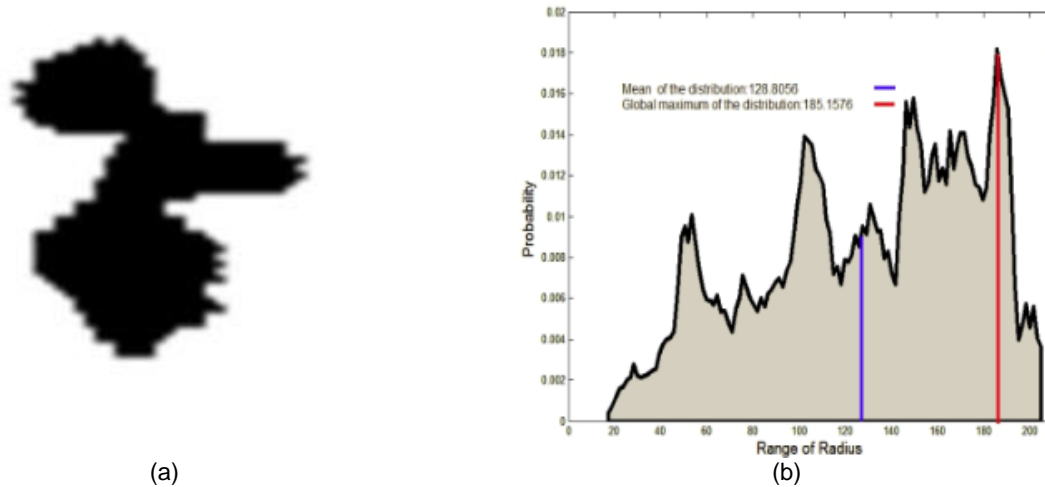


Fig. 2. Graphite nodule and its radius distribution

each border pixel and the average radius. This measure is defined as

$$MR = \frac{1}{n} \sum \frac{\bar{r}_b}{|r_j - \bar{r}_b| + \bar{r}_b}, \quad (3)$$

where r_b is the average radius from the border points to the center of the object and r_j is the radius of border point j to the center of the border. The center of the object is usually expressed as the expected point from all border points. This expression is valid only if the expected value is equal to the mean. Therefore, the average is highly correlated for closed to round objects. Consequently, this measure is not reliable to assess the roundness of irregular and partial shapes, and asymmetrical distributions.

3 A New Roundness Measure

In this section, a new roundness measure is defined.

Throughout this work it will be assumed that the distribution of the distances from the border points to the center of digital figures can be modeled as a probabilistic distribution function (pdf).

3.1 Probability Distribution Function

For practical purposes, pdf can be interpreted as the probability of occurrence of the length of certain radii. If an ideal circle is considered, where the magnitude of all radii is the same, then the pdf of the radii is composed of a single peak (see Fig. 1(a)). In contrast, when the circle is affected by noise and small shape variations, the majority of the distribution area of the radii tends to cluster around a single value. This can be observed in Fig. 1(b) where the neighborhood around the peaks becomes sparse. In this case, it is taken into consideration that the radius can be modeled as a Gaussian distribution around the radius r with σ dispersion, i.e., $r \approx G(r, \sigma)$.

However, in general, when the shape is affected by strong shape variations, the pdf becomes more complex than a single Gaussian. To illustrate this situation, Fig. 2(b) shows the pdf of the radius of an irregular graphite nodule, where it is evident that the pdf of the radius is composed of distinct peaks or modes. Therefore, the radius distribution can be modeled as mixed distributions. This model may become more complicated since there are insufficient data to estimate the set of parameters for each density function.

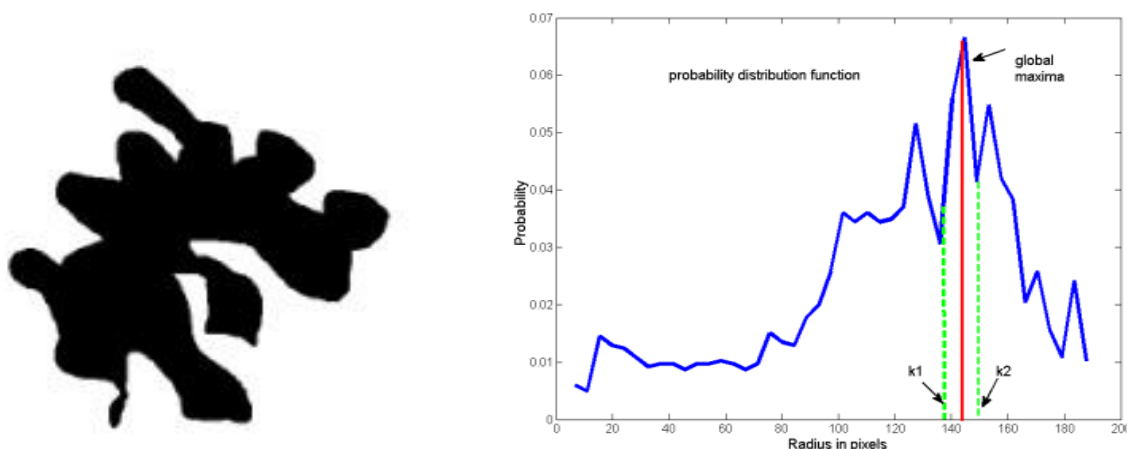


Fig. 3. Irregular object and its radius distribution

Nevertheless, a good criterion to estimate the most significant distribution consists in locating the most significant mode contained in the mixture. Hence, the aim of this article consists in determining a better radius estimator than the single average to calculate the roundness of graphite nodules that have a multimodal probability density function (mpdf).

3.2 A New Roundness Measure Based on the Probability Density Function

Based on the assumption that the pdf of the radius does not necessarily follow a Gaussian distribution (see Fig. 2), a new measure is proposed, which is based on the most significant mode of the radius distribution. Consider that if the borders of the objects have been determined, then the center of the objects is calculated from the border information by means of

$$c = E\{x_1, x_2, \dots, x_n\}, \quad (4)$$

where $\{x_1, x_2, \dots, x_n\}$ represents the set of pixels in the border and c corresponds to the expected value. Subsequently, the distances between each element of the border and the estimated center are computed as follows:

$$r = \{d_1(c, x_1), d_1(c, x_2), \dots, d_k(c, x_n)\}, \quad (5)$$

where r is the set of distances between each element of the border and the estimated center c . After determining the set of distances, its pdf expressed as $f(r)$ is computed. Next, the proportion between the area that surrounds the most significant mode (the most frequent distance from the border to the center) and the total area of the pdf are estimated. Summarizing, this is expressed as

$$MOR = \frac{\int_{k_1}^{k_2} f(r) dr}{\int_{-\infty}^{+\infty} f(r) dr}, \quad (6)$$

where the most significant mode is located in the interval $[k_1, k_2]$. The k_1 and k_2 values are determined by the maximum sparse criterion. Fig. 3 shows an example of the measure.

4 Discussion and Results

This section presents a set of experiments performed with the aim of showing the capabilities of the proposal and its behavior in synthetic and real images. In the first part, the measure is tested under a controlled scenario, where parameters such as radii and the number of sides of the digital objects generated for this case were changed. In the second part, the proposal is tested using real images.

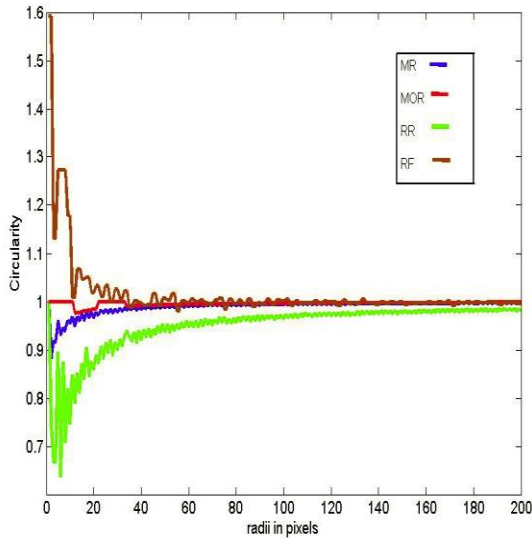


Fig. 4. Different circles artificially generated with varying radii

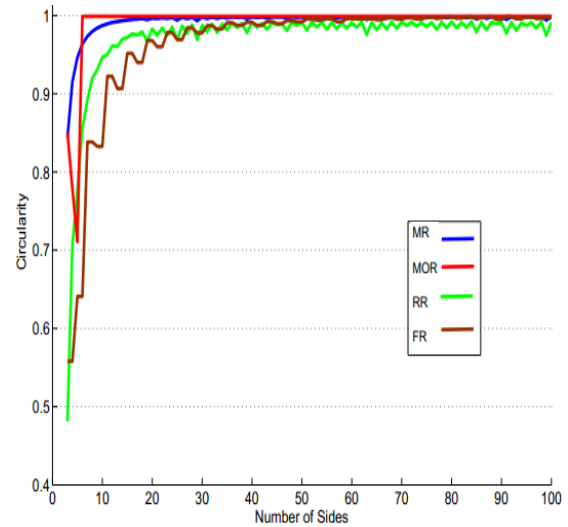


Fig. 5. Regular polygon circularity

4.1 Synthetic Images

4.1.1 Independence of Resolution

To explain the differences among the measures in terms of resolution, perfect circles were digitally drawn with radii varying from 1 to 100. Results are shown in Fig. 4. From this graphs, it can be seen that the RF measure does not maintain the basic requirements a roundness measure should have. It must range within $[0,1]$, where 1 is scored only by a perfect circle. RR and RF are the measures most affected by the resolution. As it is appreciated in red, the proposed measure converges faster with values closer to one. That is, this parameter is consistent at different resolutions. On the other hand, MOR and MR are noticeably similar, particularly, when the resolution becomes higher. The MR measure becomes numerically similar to our proposal, however, MR considers only regular shapes; therefore, it is not reliable to measure distinctive shape variations (remember that the mean does not always represent a good estimator for characterizing the roundness of an object).

4.1.2 Regular Polygon Circularity

One hundred regular polygons were generated, the number of sides ranging from 3 to 100. Fig.5 shows the circularity values when the four measures are applied. As expected, circularity increases with the number of sides and converges toward 1. The larger the number of sides is, the more the polygons look like a circle and the closer to 1 the circularity gets. Note that the MR measure is quite similar to MOR whenever the polygons are regular. However,

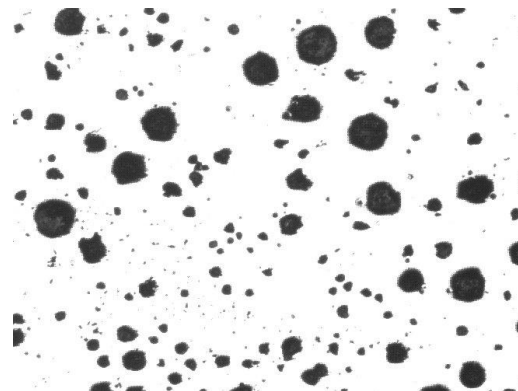


Fig. 6. Graphite specimen

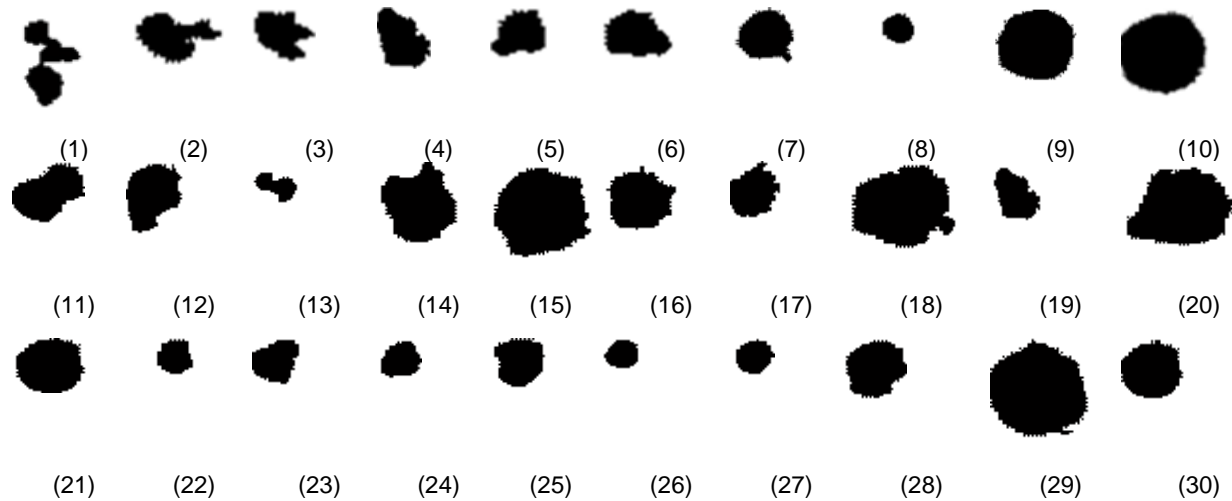


Fig. 7. Samples of graphite nodules

with respect to RR and RF, the results differ markedly.

4.2 Application in a Real Case

We are currently working in collaboration with materials specialists. They want to study the wear behavior in a ductile cast iron. The study is focused on the computation of parameters such as nodularity. Currently, the estimation of nodularity in ductile cast iron is based on how the shape of the nodules approximates to a circle. For instance, a region of graphite is more nodular when the shape of graphite nodules tends to be a circle. Ideally, the nodules should appear as circular objects in a ferritic matrix.

The image in Fig. 6 shows various morphologies of graphite particles. Microstructural images were captured with a Nikon epiphot 200 optical metallographic microscope which includes an integrated video system. The dimensions of the images are 656×494 pixels. Quantitative metallographic measurements were carried out using a $200 \times$ magnification (pixel dimension, $1.095 \mu\text{m}$).

4.2.1 Quantitative Analysis of Graphite Nodular Shapes

Table 1 and Fig. 7 show the results of different circularity measures and the illustration of each graphite specimen. Note that the specimens have different shapes: from circular shape to irregular shapes. These specimens have been selected from a randomly uniform distribution. The random population has 30 elements which warrant statistical representativeness. It looks that all measures are different, which is shown by the different indexes obtained from different specimens.

To evaluate the behavior of each measure, the distribution of the circularity measures is analyzed. Fig. 8 shows the different distribution of circularity specimens in this experiment. As it is expected, all measures provide different information about the circularity measures. However, as it can be appreciated, RR, MR and RF are grouped in a well-defined cumulus, which means that the measured specimens have a certain degree of similarity. But analyzing different elements, it is noticed that there are irregular forms (not closer to circle) to regular forms. It means that these measures do not provide a good criterion to measure the circularity. For instance, RR shows that some specimens are

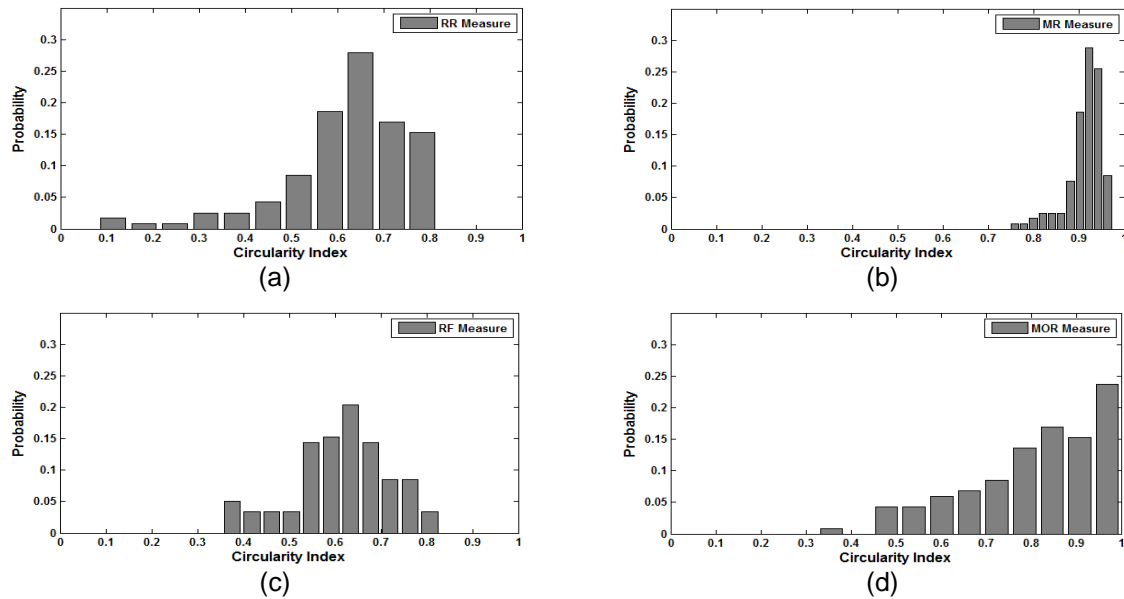


Fig. 8. Histograms of distribution of four measures: (a) RR, (b) MR, (c) RF, and (d) MOR

totally different from a circle (Fig. 8(a)), which is correct, but it also shows that there is no one close similar to a circle (the maximum circularity index is 0.8847), which is not completely true (observe the 9th specimen). MR shows the opposite: all specimens are close similar to a circle (Fig.8(b)), the majority of specimens are assigned a circularity measure close to 1, which is not true because less circular specimens have a value of about 0.6 which is sufficiently high to be considered as a non-circular shape. It means that it is possible to discriminate between the least circular nodule and the most circular one. On the other hand, RF has a better distribution of circularity measure (Fig. 8(c)). However, it indicates that rounded shapes have low values of circularity (about 0.8) and irregular shapes have high values (about 0.4). It means that in all tested measures they do not really discriminate circular shapes and do not scatter the measure uniformly in the whole domain [0, 1].

Contrary to all situations commented previously, our proposal scatters better the circularity measured from specimens analyzed (Fig. 8(d)). It can be appreciated that the index of circularity assigned to a particular specimen is more representative with its real shape, that is,

circular shapes have values close to 1, and irregular shapes close to 0. In this case, several specimens have a circularity measure close to 1 and less circular values close to 0.3, which is true when the illustration of specimens and its circularity index match. In this case, the measure distribution relates circular shapes with specimens better than the other measures and the scatterings of space allow making less and more circular shapes distinguishable.

4.2.2 Analysis of the Irregularity in Graphite Nodules

The following experiment demonstrates how the measures were affected by the irregularities in the contours.

To illustrate this, consider the nodules in Fig. 9(a) and 9(c), which are typical samples in a routine analysis in ductile cast iron production. Notice that both specimens are close to a circular shape. Alternatively, the nodules in Fig. 9(b) and 9(d) have small ragged contours. Note in Table 2 that MR, RR and RF exhibit considerable variations in the results; this means that these measures are more sensitive to irregularities in the boundaries. Therefore, the study of the dominant geometry of nodules, as it is the case in

Table 1. Estimated values of roundness for 30 segmented nodules corresponding to Fig. 7

	MOR	MR	RR	RF		MOR	MR	RR	RF		MOR	MR	RR	RF
1	0.4437	0.7563	0.0471	0.3790	11	0.5504	0.8590	0.4564	0.5665	21	0.6831	0.9488	0.7402	0.7402
2	0.5520	0.7615	0.1180	0.3502	12	0.6960	0.9027	0.5128	0.5575	22	0.8571	0.9234	0.6667	0.6153
3	0.5520	0.6315	0.5381	0.5508	13	0.5964	0.9226	0.2838	0.4558	23	0.7600	0.9083	0.5763	0.6550
4	0.5934	0.7748	0.4588	0.5508	14	0.6279	0.9253	0.6374	0.6926	24	0.6315	0.9226	0.6590	0.6753
5	0.6330	0.7803	0.6147	0.4344	15	0.7491	0.9253	0.6374	0.6926	25	0.6973	0.9422	0.6737	0.7578
6	0.6390	0.7765	0.5047	0.6620	16	0.6759	0.9453	0.7083	0.7054	26	0.8488	0.9619	0.8181	0.7630
7	0.7361	0.9424	0.6315	0.7704	17	0.7202	0.9290	0.5806	0.6359	27	0.7100	0.9474	0.7457	0.7100
8	0.9654	0.9358	0.6852	0.7756	18	0.5568	0.8997	0.5709	0.6279	28	0.6812	0.9439	0.6725	0.7194
9	0.9851	0.9661	0.8216	0.8462	19	0.5596	0.8778	0.4398	0.5596	29	0.7931	0.9583	0.7943	0.7576
10	0.9751	0.9693	0.8847	0.9080	20	0.5283	0.9000	0.5603	0.5740	30	0.7831	0.9489	0.7402	0.7211

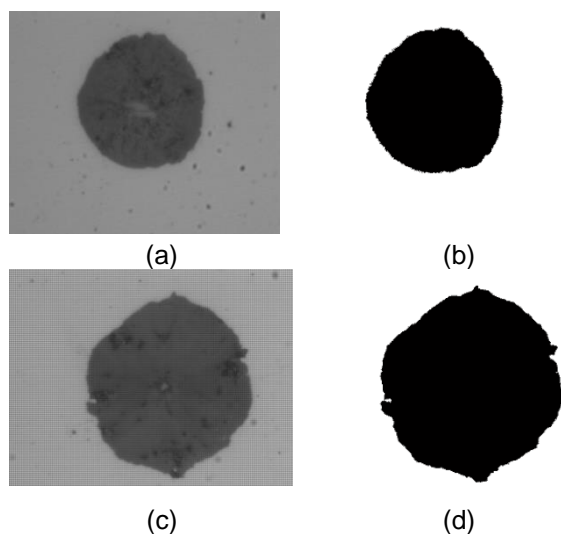


Fig. 9. (a) Circular graphite, (b) segmentation of the specimen (a), (c) circular graphite with rough boundary, and (d) segmentation of the specimen (c)

the MOR measure, will provide a more accurate parameter to study the graphite shape. This allows the possibility of efficiently measuring the roundness of the nodules even when the borders have distortions.

To demonstrate the manner in which the presence of elongated features affects the resulting measurements, perfect circles were drawn digitally (see Table 3). This comparison shows that the roundness factor (RF) is strongly affected by the presence of thin and elongated features such as lines. Besides, the maximum of Ferret's diameter is much larger than the diameter

of the inscribed circle. Consequently, when a graphite particle has a shape close to a circle, the presence of small and elongated features may render false results. To illustrate this, notice the first and the last element in Table 3, where the inaccuracy of RF dropped from 97 % to 67 %. In the same manner, RR dropped from 96 % to 0.55%. On the other hand, the values computed for MR and MOR remain approximately the same; therefore, they are not affected by the accuracy of the border.

4.2.3 Human Perception Test

To demonstrate the consistency of the measures when compared with the human perception, the nodules analyzed in Section 4.2 were evaluated

Table 2. Estimated values of roundness corresponding to specimens 8(a) and 8(c)

Graphite	MOR	MR	RR	RF
b	0.9799	0.9767	0.8752	0.9111
d	0.9413	0.9030	0.8060	0.8185

Table 3. Three digital circles with elongated features

Measures			
MOR	0.9998	0.9997	0.9890
MR	0.9955	0.9355	0.9056
RR	0.9687	0.8687	0.5503

by 30 people. In this part, each person gives a score out of a range of scores from the most circular to the least circular shape. The comparisons carried out between the participants and the measures obtained showed that MR is the least match with human perception, especially when the shape of the nodules is irregular. The main reason is that it cannot discriminate between different shapes. Another reason is that this measure is based on the average radius, which does not represent a good estimator for characterizing the roundness of irregular particles. On the contrary, with the proposed measure (MOR) it is possible to distinguish the effect of roundness. One of the reasons is that it is based on the most significant mode of the radius distribution.

The outcome of the above test demonstrates that the measure proposed by the ASTM committee (RF) is strongly affected by irregularities in the contours. As a consequence, it may easily fail, particularly, when the maximum of Ferret's diameter is larger than the diameter of the inscribed circle. Likewise, RR is affected by abrupt changes in the contours and by shape resolution. It is reasonable to expect that even when a graphite particle has a shape close to a circle, the presence of small and elongated features may render false results.

In summary, the proposed measure is more robust for computing the roundness of the graphite particles because it is capable of adapting to different scenarios, such as variations in resolution, discrepancies in contours and variations of shape.

5 Conclusions

In this article, a new quantitative method to estimate the circularity of digital objects was introduced. The proposed measure takes into consideration the dominant geometry of the objects and avoids the use of parameters such as area, perimeter and Ferret's diameter. The performance of this measure was compared with three well-known measures: the roundness factor (RF), the mean roundness (MR) and the radius ratio (RR). In the experimental analysis, we showed the robustness of the proposed measure

in different scenarios including artificial controlled scenarios and a real application; in particular, an analysis of circularity of a specimen of graphite was carried out. From the results of the present study, we concluded that the proposed measure (MOR) represents a good measure to quantify the circularity because it satisfies the following conditions: (1) it ranges within $[0,1]$, where 1 is scored only by a perfect circle, (2) it is invariant with respect to resolution, so the measure becomes independent of the equipment, (3) it is tolerant to shape variations, (4) it is tolerant with respect to noise or narrow intrusions, (5) it can be easily compared to human perception, and (6) it is easy to compute.

Acknowledgments

We would like to thank the anonymous reviewers for their valuable comments. The author Ana Marcela Herrera-Navarro thanks the government agency CONACyT (133697).

References

1. **Ahn, S.J., Rauh, W. & Warnecke H.J. (2001).** Least-squares orthogonal distances fitting of circle, sphere, ellipse, hyperbola, and parabola. *Pattern Recognition*, 34(12), 2283–2303.
2. **Almeida-Prieto, S., Blanco-Méndez, J. & Otero-Espinar, F. (2004).** Image analysis of the shape of granulated powder grains. *Journal of Pharmaceutical Sciences*, 93(3), 621–634.
3. Historical Standard: ASTM A247-67(1998) Standard Test Method for Evaluating the Microstructure of Graphite in Iron Castings.
4. **Artacho-Pérula, E., Roldán-Villalobos, R., Martínez-Cuevas J.F., & López-Rubio, F. (1994).** Nuclear quantitative grading by discriminant analysis of renal cell carcinoma samples: a patient survival evaluation. *The Journal of Pathology*, 173(2), 105–114.
5. **Bose, P. & Morin, P. (2003).** Testing the quality of manufactured disks and balls. *Algorithmica*, 38(1), 161–177.
6. **Bottema, M.J. (2000).** Circularity of objects in images. *2000 IEEE International Conference on Acoustics, Speech and Signal Processing (ICASSP'00)*. Istanbul, Turquia, 4, 2247–2250.

7. **Bouwman, A.M., Bosma, J.C, Vonk, P., Wesselingh, J.A. & Frijlink, H.W. (2004).** Which shape factor (s) best describes granules? *Powder Technology*, 146(1-2), 66–72.
8. **Cenens, C., Jenné R. & Van. I.J. (2002).** Evaluation of different shape parameters to distinguish between flocs and filaments in activated sludge images. *Water Science Technology*, 45(4-5), 85–91.
9. **Chaudhuri, D. (2010).** A simple least squares method for fitting of ellipses and circles depends on border points of a two-tone image and their 3-D extensions. *Pattern Recognition Letters*, 31(9), 818–829.
10. **Chatzis, V., Kaburlasos, V.G., & Theodorides, M. (2005).** An image processing method for particle size and shape estimation. *2nd International Scientific Conference on Computer Science*, Chalkidiki, Greece, 7–12.
11. **Chen, M.C. (2002).** Roundness measurements for discontinuous perimeters via machine visions. *Computers in Industry*, 47(2002), 185–197.
12. **Dasgupta, A. & Lahiri, P. (2000).** Digital indicators for red cell disorder. *Current Science*, 78(10), 1250–1255.
13. **De Santis, A., Di Bartolomeo, O., Iacoviello, D., & Iacoviello, F. (2008).** Quantitative shape evaluation of graphite particles in ductile iron. *Journal of Materials Processing Technology*, 196(1-3), 292–302.
14. **Di Ruperto, C. & Dempster, A. (2000).** Circularity measures based on mathematical morphology. *Electronics Letters*, 36(20), 1691–1693.
15. **Foresto, P., D'Arrigo, M., Carreras, L., Cuzzo, R.E., Valverde, J. & Rasia, R. (2000).** Evaluation of red blood cell aggregation in diabetes by computerized image analysis. *Medicina (B. Aires)*, 60(5 pt. 1), 570–572.
16. **Frosio, I. & Borghese, N.A. (2008).** Real time accurate circle fitting with occlusions. *Pattern Recognition*, 41(3), 1041–1055.
17. **Giger, M.L., Doi, K., & MacMahon, H. (1988).** Image feature analysis and computer-aided diagnosis in digital radiography, automated detection of nodules in peripheral lung fields. *Medical Physics*, 15(2), 158–166.
18. **Gordon, A., Colman-Lerner, A., Chin, T.E., Benjamin, K.R., Yu, R.C., & Brent, R. (2007).** Single-cell quantification of molecules and rates using open-source microscope-based cytometry. *Nature Methods*, 4(2), 175–181.
19. **Hawkins, A.E. (1993).** *The shape of powder-particle outlines*. Taunton: Research Studies Press.
20. **Hetzner, D.W. (2008).** Comparing binary image analysis measurements-euclidean geometry, centroids and corners. *Microscopy Today*, 16(4), 10–15.
21. **Hilaire, X. & Tombre, K. (2006).** Robust and accurate vectorization of line drawings. *IEEE Transactions on Pattern Analysis and Machine Intelligence*, 28(6), 890–904.
22. **Kovalevsky, V.A. (1990).** New definition and fast recognition of digital straight segments and arcs. *10th International Conference on Pattern Recognition*, Atlantic City, NJ, 2, 31–34.
23. **Li, J., Lu, L., & Lai, M.O. (2000).** Quantitative analysis of the irregularity of graphite nodules in cast iron. *Materials Characterization*, 45(2), 83–88.
24. **Liew, L.H., Lee, B.Y. & Chan, M. (2010).** Cell detection for bee comb images using circular Hough transformation. *2010 International Conference on Science and Social Research (CSSR)*, 191–195.
25. **Mohler, J.L., Partin, A.W., Epstein, J.I., Lohr, W.D., & Coffey, D.S. (2008).** Nuclear roundness factor measurement for assessment of prognosis of patients with prostatic carcinoma. Standardization of methodology for histologic sections. *The Journal of Urology*, 139(5), 1085–1090.
26. **Montero, R.S. (2009).** State of the Art of Compactness and Circularity Measures. *International Mathematical Forum*, 4(27), 1305–1335.
27. **Morales-Hernández, L.A., Terol-Villalobos, I.R., Domínguez-González, A., Manriquez-Guerrero, F., & Herrera-Ruiz, G. (2010).** Spatial distribution and spheroidicity characterization of graphite nodules based on morphological tools. *Journal of Materials Processing Technology*, 210(2), 335–342.
28. **Peura, M. & Iivarinen, J. (1997).** Efficiency of simple shape descriptors. *3^d International Workshop on Visual Form, Capri, Italy*.
29. **Pegna, J. & Guo, C. (1998).** Computational metrology of the circle. *Proceedings of Computer Graphics International*, Hannover, Germany, 350–363.
30. **Ritter, N. & Cooper, J. (2009).** New resolution independent measures of circularity. *Journal of Mathematical Imaging and Vision*, 35(2), 117–127.
31. **Roussillon, T., Sivignon, I., & Tougne, L. (2010).** Measure of circularity for parts of digital boundaries and its fast computation. *Pattern Recognition*, 43(1), 37–46.

32. **Sauer, P. (1993).** On the recognition of digital circles in linear time. *Computational Geometry*, 2(5), 287–302.
33. **Swanson, K., Lee, D.T., & Wu, V.L. (1995).** An optimal algorithm for roundness determination in convex polygons. *Computational Geometry*, 5(4), 225–235.
34. **Nguyen, T.P. & Debled-Rennesson, I. (2010).** Circularity Measure in Linear Time. *20th International Conference on Pattern Recognition (ICPR 2010)*, Istanbul, Turkey, 2098–2101.
35. **Yip, R.K.K., Tam, P.K.S., & Leung, D.N.K. (1992).** Modification of Hough transform for circles and ellipses detection using a 2-dimensional array. *Pattern Recognition*, 25(9), 1007–1022.
36. **Pan, L., Chu, W.-S., Saragih, J.M., & De la Torre, F. (2012).** Fast and Robust Circular Object Detection with Probabilistic Pairwise Voting. *IEEE Signal Processing Letters*, 18(11), 639–642.
37. **Worring, M. & Smeulders, A.W.M. (1995).** Digitized circular arcs: characterization and parameter estimation. *IEEE Transactions on Pattern Analysis and Machine Intelligence*, 17(6), 587–598.
38. **Žunić, J., Hirota, K., Rosin, P.L. (2010).** A Hu moment invariant as a shape circularity measure. *Pattern Recognition*, 43(1), 47–57.



Ana M. Herrera-Navarro received the B.S. degree in Computer Engineering and her M.S. degree in Computer Science from Informatics Faculty of the Queretaro Autonomous University, Mexico. She is currently a Ph.D. student at the Queretaro Autonomous University. Her research interests include morphological image processing and computer vision.



Hugo Jiménez Hernández received the B.S. degree in Computer Science Engineering at the Queretaro Regional Technological Institute; his M.S. in Computer Science at the Center

for Computing Research of National Polytechnic Institute (IPN), Mexico. He received his Ph.D. degree from CICATA Queretaro-IPN. His research includes automatic activities detection, associative memories and time series analysis.



Hayde Peregrina-Barreto received her B.S. in Computer Engineering from Cuautla Institute of Technology, Mexico, and her M.S. in Electrical Engineering from the Guanajuato University, Mexico. She received her Ph.D. degree from UAQ. Her research interests include morphological image and computer vision.



Federico Manríquez-Guerrero received his B.S. in Metallurgical Engineering and Chemistry from the Autonomous University of Mexico (UNAM); his M.S. in Metallurgy from UNAM. He is a researcher at CIDETEQ, Mexico. His current research interests include morphological image processing and materials characterization.



Iván R. Terol-Villalobos received his B.S. from National Polytechnic Institute (IPN), Mexico; his M.S. in Electrical Engineering from the Center for Research and Advanced Studies of IPN, Mexico, and a DEA in Computer Science from the University of Paris VI, France. He is currently a researcher at CIDETEQ, Mexico. His current research interests include morphological image processing, morphological probabilistic models and computer vision.

Article received on 02/02/2012; accepted on 23/01/2013.